

# DESIGN AND OPTIMIZATION OF HYBRID ED-RO SYSTEMS FOR THE TREATMENT OF HIGHLY SALINE BRINES

**Authors:** *Ronan K. McGovern, Syed M. Zubair, John H. Lienhard V*

**Presenter:** Ronan Killian McGovern  
PhD Candidate – Massachusetts Institute of Technology – U.S.A.  
mcgov@mit.edu

## **Abstract**

The demand is rising for desalination technologies to treat highly saline brines arising from hydraulic fracturing processes and inland desalination. Interest is growing in the use of electrical desalination technologies for this application. The hybridization of electrodialysis (ED) with reverse osmosis (RO) allows high salinities (beyond the range of RO alone) to be reached while avoiding the operation of ED with a low conductivity diluate stream. Such hybrid systems have been experimentally investigated for concentrates from brackish and seawater desalination. However, progress is required in the modelling and optimization of hybrid systems at higher concentrations. A novel hybrid arrangement of counterflow ED systems with reverse osmosis is presented to concentrate a saline feed at 120 ppt. The system is considered from the perspective of efficiency, membrane productivity and the levelised cost of water, with emphasis on the optimisation of current density. In contrast to brackish ED systems, membrane resistances are found to dominate diluate and concentrate resistances at high salinity. The current density found to minimise LCW (levelised cost of water) is significantly greater than the current density found to maximise efficiency, indicating the high current capital cost of ED per unit membrane area and poor membrane transport properties relative to RO. Finally, performance at high recoveries is found to be limited by high stream-to-stream concentration differences, increasing water transport via osmosis, decreasing efficiency and increasing the LCW.



## I. INTRODUCTION

### 1.1 Motivation

Reverse osmosis (RO) has demonstrated great success in the desalination of seawater over the past decade, accounting for over 80% of total contracted capacity in 2010 and 2011 [1]. However, its ability to treat waters of higher salinity is limited by the hydraulic pressure allowable within pressure vessels. Meanwhile, the volume of highly saline brines produced in the world is increasing rapidly. Disposal of concentrated brines from inland desalination and produced water in the oil and gas industry is a growing issue [2,3]. Energy efficient, low cost technologies to recover water and salts from concentrated streams are needed.

### 1.2 Literature Review

Korngold et al. [4] investigated a batch electrodialysis (ED) system for volume reduction of a brackish water reverse osmosis concentrate stream (containing silica and gypsum). Concentrate of 1.5% salinity was fed to the ED system and concentrated to approximately 10%. Gypsum was precipitated from the concentrate stream in an adjacent precipitation unit. Oren et al. [5] operated a continuous ED-RO process whereby the concentrated stream from a 2<sup>nd</sup> stage RO unit was fed to the diluate side of the ED unit and recirculated to the feed side of the first RO stage. TDS of 10,000 ppm was achieved within the continuously circulated ED concentrate side while simultaneously crystalizing solids within a side loop crystallizer.

Thampy et al. [6] evaluated a continuous ED process with the ED diluate stream flowing for final treatment to an RO unit and the RO concentrate being recirculated to the ED feed. The concentrate concentrations achieved by the ED unit were lower than that of Oren et al. due to the once-through flow path on the concentrate side of the ED unit. Casas et al. [7] investigated batch concentration of RO concentrate, finding the concentration of sodium chloride achievable to be limited by back diffusion and electro-osmotic transport. As remarked by Casas et al. [7], further analysis of energy consumption and process optimization is required for hybrid ED-RO systems. This is the gap this research aims to address.

### 1.3 Goals

By hybridizing electrodialysis with reverse osmosis, higher salinity feeds may be treated than with RO alone, while the use of RO avoids operation of ED with streams of low conductivity. This study outlines the design of a desalination system consisting of counterflow ED units hybridised with RO. In particular, the following tasks are the focus of this work:

- Modelling of the efficiency, membrane productivity and levelised cost of water (LCW) of this hybrid system
- Determination of the current density maximising the LCW and the efficiency.

The design of the ED systems rather than the RO system is emphasised. An RO system design typical of a single stage single pass seawater RO (SWRO) is assumed. Furthermore, to limit the scope of this work, the design and optimisation of ED pumping systems is overlooked, though important in eventually determining and optimizing overall system costs.

## II. DESIGN CONSIDERATIONS FOR ED AT HIGH SALINITY

The design of electrodialysis systems for the desalination of high concentration solutions is notably different than brackish water electrodialysis or indeed electrode-ionisation. In particular, the limiting

current density and concentration polarization are no longer limiting at higher concentrations. Instead the balance between ohmic losses and losses due to water transport via electro-osmosis and osmosis becomes central in design.

### 2.1 Relative importance of ohmic losses in solutions and membranes

In brackish water ED, ohmic losses within the diluate stream are very significant due to low conductivity. It is useful to compare the ohmic resistance of the diluate stream, Eq. 1, and the ohmic resistance of typical cation and anion exchange membranes. Neosepta anion and cation exchange membranes are considered with surface resistances of 2.4 and 3  $\Omega \text{ cm}^2$  respectively [17].

$$\text{Eq. 1 } \bar{r}_d = \frac{h_d}{\Lambda_d C_d}$$

Here,  $\bar{r}_d$  is the surface resistance of the diluate in  $\Omega \text{ m}^2$ ,  $h_d$  is the diluate channel spacing in m,  $\Lambda_d$  is the molar conductivity of the diluate stream in  $\text{S m}^2/\text{mol}$ , and  $C_d$  is the diluate concentration in  $\text{mol}/\text{m}^3$ . Figure 1 illustrates the ohmic resistance of the diluate stream relative to the ohmic resistance of the membranes. Experimental data relating conductivity and NaCl concentration is interpolated to calculate the molar conductivity [11] of the diluate stream in Eq. 1. For diluate channel spacings even up to 2.5 mm, membrane resistances dominate at concentrations above approximately 1 mol/L. Overall ohmic resistance of the stack is significantly less sensitive to changes in concentration of the diluate and concentrate streams for high salinity ED applications. For desalination to concentrations that meet drinking water standards (<500 ppm), however, the benefit of hybridization with RO is to avoid high stack resistances encountered at low concentrations.

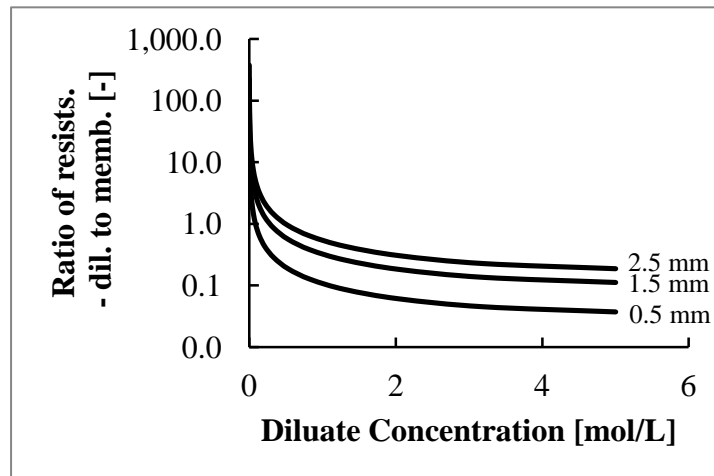


Figure 1. Ratio of diluate to membrane channel resistance

### 2.2 Limiting current density and concentration polarization

In low salinity applications, the limiting current density hinders the quantity of salt that may be removed per unit of membrane area. In essence, this limit upon the rate of ion removal occurs as ion diffusion towards the membrane surface becomes insufficient to replenish the concentration of salt at membrane-solution interfaces. The physics observed in this regime of operation is complex and analysed in detail in literature [8, 9].

In high salinity applications, the concentration of salt in the diluate and concentrate streams is large enough for the depletion of ions at the membrane-solution interface to occur only at very high current densities. Furthermore, the impact of concentration polarization is relative to a much larger

difference in concentration between the diluate and concentrate streams, i.e. higher levels of concentration polarization may be tolerated. Considering a balance between convection and diffusion within a film adjacent to a membrane, the extent of concentration polarization on the diluate side of each membrane may be estimated employing Eq. 2 [10].

$$\text{Eq. 2 } \frac{\Delta C}{\Delta x} \approx -\frac{i(T_i^d - t_i^m)}{z_i F D_s}$$

Here,  $i$  denotes the current density,  $F$  Faraday's constant,  $T_i^d$  the transport number of ion  $i$  in the diluate and  $t_i^m$  the apparent transport number of ion  $i$  in the membrane. Although  $D_s$ , the electrolyte diffusivity, is affected by the current density and by solution concentration, we may approximate a lower bound on its value by considering the self-diffusion coefficient of a dilute NaCl solution at zero current density [11]. The value of the effective transport number of the co-ion in a membrane is typically close to one. For the desalination of NaCl solutions, concentration polarization is higher at the cation exchange surface according to Eq. 2, since the transport number of sodium in solution is lower than chloride (sodium has a larger hydration shell causing greater drag). The transport number for sodium in solution is estimated from the diffusivity and viscosity of pure water, Table 1.

**Table 1: Concentration polarization estimation**

Symbol	Value	Ref.
$D_s$	$1.61 \times 10^{-9} \text{ m}^2/\text{s}$	[11]
$T_i^d$	1	Assumed
$t_{Na}^m$	0.396	Calculated <sup>1</sup>
$\nu$	$8.9 \times 10^{-7}$	[12]
$Sc \approx \frac{\nu}{D_s}$	580	Calculated
$Re$	25	[13]

To estimate the gradient of concentration in Eq. 2, a relation for flow within a meshed channel is required, and it is provided by Eqs. 3 and 4, valid for  $10 < Re < 25$  [13].

$$\text{Eq. 3 } \frac{\Delta C}{\Delta x} = \frac{\Delta C}{D_h} Sh$$

$$\text{Eq. 4 } Sh = 0.53 Re^{\frac{1}{2}} Sc^{\frac{1}{3}}$$

Here,  $D_h$  is the hydraulic diameter of the channel spacing,  $Sh$  is the Sherwood number,  $Re$  is the Reynolds number, and  $Sc$  is the Schmidt number, the ratio of momentum diffusivity,  $\nu$ , to mass diffusivity,  $D$ . Figure 2 illustrates the degree of concentration polarization at the diluate side surface of a cation exchange membrane in contact with an NaCl solution. For a small membrane spacing the concentration polarization can be small relative to stream-to-stream concentration differences. For larger membrane spacings concentration polarization is a significant effect beyond current densities of approximately  $500 \text{ A/m}^2$ . Importantly, the conclusions drawn are all contingent upon the Reynolds number and the diluate channel gap. Although not within the scope of this work, the optimization of

<sup>1</sup> Employing the limiting diffusivities of sodium and chloride

these parameters in accordance with the trade-off between polarization effects and pumping power requirements is important.

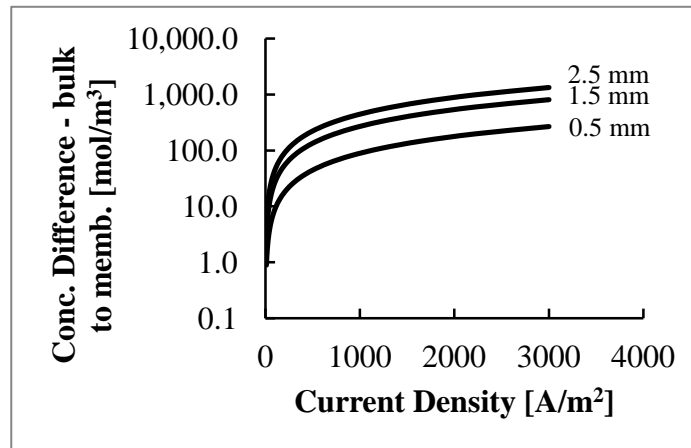


Figure 2. Concentration difference due to concentration polarization at a Reynolds of 25

Concentration polarization affects ED performance in three significant ways, which are only briefly described here:

1. Solution resistance increases within diluate stream boundary layers, although the impact upon overall resistance is less significant in high concentration ED systems.
2. Concentrations at the solution-membrane interface are decreased in the diluate and increased in the concentrate, causing an increase in the minimum potential required for desalination.
3. Potential differences, known as junction potentials [14], occur across the concentration polarization layers as a result of concentration gradients.

### 2.3 Maximum concentration achievable in electro dialysis

The ability of electro dialysis to produce a high concentration concentrate is limited by electro-osmotic transport from the diluate to the concentrated stream. This transport of water results from ions passing from the diluate to the concentrate and dragging a quantity of water with them, through the membrane. The ratio of the number of moles of water transported to the number of moles of ions is denoted the water transport number. Thus, the maximum concentration achievable,  $c_{max}$ , in concentrating a sodium chloride solution depends upon the water transport numbers of the sodium and chloride ions in the cation and anion exchange membranes respectively [13]:

$$\text{Eq. 5 } c_{max} = \frac{1}{(1+t_{w,Na}+t_{w,Cl})\bar{v}_{sol}}$$

Here,  $\bar{v}_{sol}$  is the molar volume of the solution. In low salinity applications, the effective concentration of a volume containing an ion with water transported remains significantly above the concentration of the concentrated stream. However, where the salinity of the concentrate is high, the effective concentration of this volume transported can be similar in value. The modelling of electro-osmotic transport through membranes is complex and depends upon the degree of crosslinking of the membrane (related to pore and channel size and distributions) and also the concentration of the diluate and concentrated solutions [15]. To some extent, in particular at high concentrations, the water transport number is related to the hydration number of the ion in a concentrated solution [15].

For large differences between concentrate and diluate concentrations, water transport due to osmosis becomes very significant. More specifically, the loss in Gibbs free energy due to the osmotic transport of water from the diluate to the concentrate stream becomes large relative to the increase in free energy achieved in moving salt from the diluate to the concentrated stream. Losses due to osmosis may be reduced relative to the desirable change of free energy associated with desalination by increasing the current density. However, increases in current density come at the expense of increased ohmic losses. Consequently, there exists a balance between losses due to osmosis and losses due to ohmic resistances (see results).

With improved models for water transport, it would be possible, during system design, to consider the trade-offs between electro-osmotic losses and other losses within the system. Furthermore, it should be possible to develop membranes with properties that optimize system performance. For now, we only recognize that electro-osmosis limits the maximum concentration achievable with ED and consider values obtained experimentally in system testing of ED concentration.

#### 2.4 Summary of high salinity ED

ED desalination at high salinity exhibits three distinctive characteristics:

1. The overall ohmic resistance of the stack is insensitive to changes in diluate or concentrate concentration. Membrane resistances dominate.
2. For small channel spacings, the degree of concentration polarization can be small relative to stream-to-stream concentration differences. The true impact of concentration polarization can only be clarified in the context of an optimization of the pumping system, channel width and Reynolds number.
3. The maximum concentration achievable is limited by electro-osmotic transport of water but also by transport via osmosis. As shall be seen in Sect. VI, the trade-off between membrane ohmic losses and losses associated with water transport is central in optimizing efficiency and the levelised cost of water (LCW).

### III. SYSTEM DESCRIPTION AND MODELLING

Figure 3 illustrates the hybrid ED-RO system configuration. The purpose of ED system A is to concentrate a portion of feed water to the desired concentrate concentration whilst diluting the remainder towards the concentration of the feed to the RO unit. ED system B serves the purpose of diluting concentrate from the RO system (along with the diluate of ED system A) to a concentration amenable to treatment with RO. ED system B also produces a concentrate at the same concentration as the feed water, allowing it to be recycled and treated by ED system A.

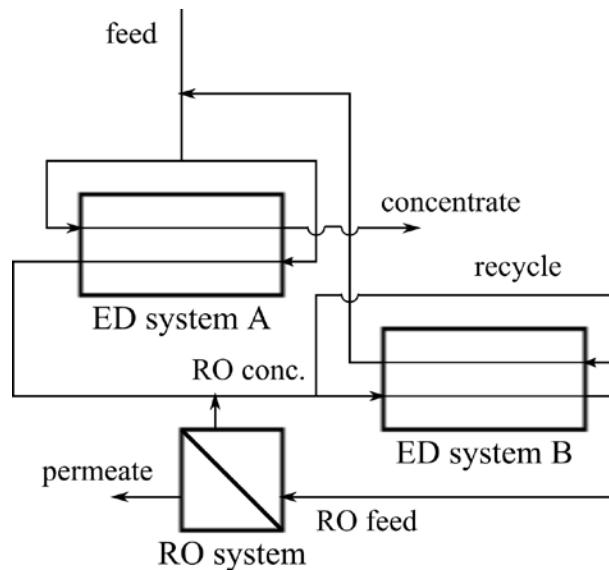


Figure 3. Schematic diagram of the hybrid ED RO system

Both ED systems are envisioned to operate in a counter-flow arrangement. Such an arrangement allows a significant difference in concentration to be maintained between the diluate and concentrate streams. This is in contrast to a co-flow arrangement where streams would necessarily be at the same concentration in the inlet to system A. The maintenance of such a difference in concentration is important to ensure that each unit of membrane area achieves a significant rise in the free energy of salt (the desirable result of the desalination process). Were concentrations to be close, energy is expended while moving salt between streams of very similar concentration.

In the present analysis, the design of an RO unit is chosen to be typical of a SWRO unit, taking a feed of 35 ppt and producing a concentrate at 70 ppt (constituting a recovery ratio for the unit of 50%).

The following key assumptions are involved in the analysis:

- Focus is maintained upon the efficiency of the system and the membrane area required. Though important, the optimization of the pumping system is outside of the analysis' scope.
- Channel spacings are assumed to be sufficiently small for the effects of concentration polarization to be negligible.
- In practice, ED systems A and B would consist of multiple stages. Here, they are each modelled as single stages.
- Electrode potentials are neglected relative to the voltage drop across cell pairs.

### 3.1 Evaluation of Donnan potentials

On the surface of each membrane, a thin region, orders of magnitude thinner than concentration polarization layers, and known as the electrical double layer, is present, within which electro-neutrality is not satisfied. An electrical potential exists across these double layers to compensate for the difference in chemical potential between species in the electro-neutral solution and within the membrane. Due to the differences in chemical potential of species in the bulk solution on either side of a membrane (associated with concentration differences) the overall effect of the Donnan potentials on either side of the membrane is to cause a net electrical potential across the membrane, denoted with  $m$  for membrane potential. For a membrane with ideal counter-ion permselectivity the membrane potential is given by:

$$\text{Eq. 6} \quad E_m = \frac{RT}{z_- F} \ln \left( \frac{a_{NaCl,c}}{a_{NaCl,d}} \right)$$

Here,  $a$  denotes the activity of a species (in this case NaCl),  $R$  is the ideal gas constant,  $T$  is ambient temperature, and  $z_-$  denotes the anion charge number. For non-ideal membranes in which the current is not solely carried by the counter ion (i.e. where the counter-ion transport number is less than unity), the membrane potential is lower than the ideal value. The convection of water via osmosis and electro-osmosis, and the diffusion of ions within the membrane influence the membrane potential to a lesser extent. A review of such effects is provided by Helfferich [16]. Here, we shall satisfy ourselves with the first order accuracy provided by Eq. 6.

### 3.2 Evaluation of solution resistances

Both the diluate and concentrate solutions flow through a mesh spacer within their respective channels. For the purpose of modeling, these solutions are considered to be well mixed with a uniform conductivity throughout the channel. The ohmic resistances of these solutions, based upon unit area (i.e.  $\Omega \text{ m}^2$ ) is given by Eq. 7:

$$\text{Eq. 7} \quad \bar{r}_l = \frac{h_l}{\Lambda_l c_l}$$

where  $\Lambda_l$  is the molar conductivity of the concentrate or diluate solution and is a function of salinity [11], and  $c_l$  is the concentrate or diluate concentration in  $\text{mol/m}^3$ . A channel width of 0.5 mm is assumed in the subsequent calculations.

### 3.3 Membrane properties

A summary of experimental measurements of membrane resistances, water permeability, salt permeability and overall water transport number from the literature are provided in Table 2.

**Table 2: ED Membrane Properties**

Symbol	Value	Ref.
$\bar{r}_{am}$	$2.4 \times 10^{-4} \Omega \text{ m}^2$	[17]
$\bar{r}_{cm}$	$3 \times 10^{-4} \Omega \text{ m}^2$	[17] <sup>2</sup>
$t_w$	10.08	[18]
$L_w$	$7.09 \times 10^{-6} \text{ m s}^{-1}$	[18] <sup>2</sup>
$L_s$	$1.38 \times 10^{-8} \text{ m s}^{-1}$	[18]

Of importance is the relevant magnitude of the salt diffusion coefficient and permeability of the membrane to water. It is unsurprising that the diffusion coefficient for salt should be lower since co-ions are strongly rejected by the membrane. As a consequence of electro-neutrality, the diffusion of ions is rendered difficult. As a simplifying assumption, salt transport via diffusion is neglected as losses associated with water transport through osmosis dominate.

### 3.4 ED System Modelling

<sup>2</sup> Converted from units of  $\text{mol/ bar m}^2 \text{ s}$



ED systems A and B are modelled via finite difference equations for a single cell pair, allowing the voltage and hence the power consumption in each finite difference to be evaluated. Conservation of salt and of total mass within each finite difference is employed for the concentrate and diluate streams within each unit. Salt and water transport from the diluate to the concentrate channel are described by Eqs. 8 and 9:

$$\text{Eq. 8 } j_s = i/F$$

$$\text{Eq. 9 } j_w = t_w j_s + L_w (C_c - C_d)$$

Here  $j$  indicates a molar flux in mol/m<sup>2</sup> s and  $L_w$  the water permeability in m/s. The overall voltage across a differential element of one cell pair during each time step is given by a sum of the membrane and solution surface resistances along with the membrane potential:

$$\text{Eq. 10 } \Delta V_{cp}[k] = i(\bar{r}_{ma} + \bar{r}_{ma} + \bar{r}_d[k] + \bar{r}_c[k]) + \Delta E_m[k]$$

Here,  $\bar{r}_{ma}$  indicates a membrane surface resistance, in this case of the anion exchange membrane, in  $\Omega$  m<sup>2</sup>.  $k$  is an index in space for the elements. Instantaneous power consumption is computed via the product of cell pair voltage, current and the area of the differential cell pair element area:

$$\text{Eq. 11 } P[k] = \Delta V_{cp}[k] i \delta A_m$$

where  $\delta A_m$  is the area of a cell pair increment. Summing over the index  $k$ , the total power (for all cell increments) may be computed.

### 3.5 RO model specifications

A simple RO model is employed with membranes producing an average permeate flux of 13 L/m<sup>2</sup>h [19]. The RO membrane is assumed to have perfect salt rejection and a permeability of 0.31 L/(m<sup>2</sup> h bar) [19]. Pressure drop due to viscous effects in the feed channel and concentration polarization are both neglected. A finite difference model (with 20 finite differences) is employed to model permeate flux along membrane pressure vessels. Salinity at the inlet to each finite difference is calculated via the conservation of salt in the concentrate stream:

$$\text{Eq. 12 } S_{c,RO}[k] \dot{m}_{c,RO}[k] = S_{c,RO}[k+1] \dot{m}_{c,RO}[k+1]$$

Here,  $\dot{m}$  is a mass flow rate in kg/s. Osmotic pressure,  $\Pi$ , in bar, in each cell is calculated at the cell's inlet salinity using Eq. 13.

$$\text{Eq. 13 } \Pi[k] = \frac{RT}{v} v_{NaCl} m_{RO,c} (S_{RO,c}) \phi(S_{RO,c})$$

Here,  $\phi$  is the osmotic coefficient and  $m$  is the solute molality in mol solute/kg solvent. The 1-dimensional finite difference model solves the following equation in each cell, with  $A_m$  the membrane permeability and  $j_w$  the water flux:

$$\text{Eq. 14 } j_{w,RO}[k] = A_m (P - \pi[k])$$

These equations are solved iteratively in combination with equations describing the ED system to evaluate the inlet hydraulic pressure to the RO unit and the membrane area required. In computing power consumption the pump efficiency,  $\eta_p$ , is assumed to be 75% and no pressure recovery device is employed. Work per unit of permeate is thus described by Eq. 15:

$$\text{Eq. 15 } w_{RO} = \frac{P\dot{m}_{f,RO}}{\eta_p \rho_{f,RO} \dot{m}_{p,RO}}$$

Here,  $w_{RO}$  denotes work done in J per kg of RO permeate,  $p$  is the pressure in Pa of the feed and  $\rho_{f,RO}$  is the feed density in kg/m<sup>3</sup>.

### 3.6 Physical Properties

The salt considered is sodium chloride. Data relating the osmotic coefficient, salt activity coefficient and electrolyte conductivity were taken from Robinson and Stokes [11] while density was taken from Busey [20].

### 3.7 Solution of hybrid system equations

In addition to parameters described in Sect. 3.4 and 3.5, the following constraints are applied in solving the coupled systems of equations for the ED systems and the RO system.

- Feed salinity to the entire system is set at 120 ppt.
- The volume flow rate of permeate from the entire system is set at 100 m<sup>3</sup>/day.
- The relative mass flow rate at the inlet to the diluate and concentrate compartments in system A is set such that the stream-to-stream concentration differences at either end of the unit are equal. This condition is also imposed in system B. This is to promote a constant current density within the stages of systems A and B.
- The current densities within units A and B are chosen in accordance with the optimization to be described in Section 4.
- Mass conservation equations are employed at nodes of intersection of streams in Fig. 3.
- For clarity and ease of comparison, all energetic quantities are calculated on the basis of unit permeate production of the RO unit. Each of ED system A, system B and the RO unit can be seen as contributing to the total energy required to produce each unit of permeate.

Solving the entire system of equations yields the power consumption of each unit, the membrane area of each unit, the concentrate stream concentration and the overall recovery ratio of the system.

## IV. MINIMISATION OF THE LEVELISED COST OF WATER

Minimisation of the levelised cost of water requires an understanding of how energy requirements and system size scale with current density. In this simplified analysis, energy is costed on the basis of \$/kWh,  $K_E$  and capital equipment is costed on the basis of \$/m<sup>2</sup> cell pair area,  $K_C$ .

For a defined process of desalination, where mass flow rates and salinities of the feed, concentrate and product are fixed, the required change in Gibbs free energy of the streams, known as the reversible work, may be determined. Knowing the Second Law efficiency of the system,  $\eta$ , the total work required may be computed by dividing the reversible work by the efficiency, Eq. 17. Likewise, knowing the average membrane productivity of the system,  $\xi$ , defined as rate of reversible work per unit of

membrane area, the total membrane area may be computed by dividing the reversible work by the membrane productivity, Eq. 18.

$$\text{Eq. 17 } \eta = \frac{\frac{RT}{F} \left[ i \ln \left( \frac{a_{NaCl,c}}{a_{NaCl,d}} \right) - it_w \ln \left( \frac{a_{w,c}}{a_{w,d}} \right) - L_w (C_c - C_d) \ln \left( \frac{a_{w,c}}{a_{w,d}} \right) \right]}{iV_{cp}}$$

$$\text{Eq. 18 } \xi = \frac{RT}{F} \left[ i \ln \left( \frac{a_{NaCl,c}}{a_{NaCl,d}} \right) - it_w \ln \left( \frac{a_{w,c}}{a_{w,d}} \right) - L_w (C_c - C_d) \ln \left( \frac{a_{w,c}}{a_{w,d}} \right) \right]$$

Second Law efficiency is defined as the rate of change of free energy to the rate of work input, both per unit of membrane area. The rate of change of free energy is equal to the rate of increase of free energy of the salt when transported from the diluate to the concentrate minus the rate of change of free energy associated with water transport from the diluate to the concentrated stream. The rate of work input is simply the product of the current density times the cell pair voltage. The membrane productivity is the net change in free energy per unit of membrane area, i.e. the numerator of the efficiency.

The contribution of each system,  $i$ , to the levelised cost of water is calculated by combining the amortised capital costs of the system with the cost of energy, Eq. 19.

$$\text{Eq. 19 } LWC_i \left[ \frac{\$}{m^3 \text{ product}} \right] = \frac{r}{\left[ 1 - \left( \frac{1}{1+r} \right)^T \right]} \frac{w_i^{rev}}{3.16E7 \frac{s}{yr} \cdot CF \cdot \xi_i} K_C + \frac{w_i^{rev}}{\eta_i} \left( \frac{K_E}{3.6E6 \frac{kWh}{J}} \right)$$

where  $r$  is the return on capital invested,  $T$  is the system life in years,  $CF$  is the capacity factor and  $w_{rev}$ , in  $J/m^3$ , is defined as the reversible work done in system  $i$  per unit of product produced by the entire hybrid system.  $w_{rev}$  is calculated considering the mass flow rates and concentrations of streams entering and exiting units A and B. This must be done via an iterative process specifying the current density in Systems A and B to estimate  $w_{rev}$  and then updating the current density based on cost considerations. Choosing representative values for the concentrate and diluate concentrations in ED systems A and B, Eq. 17, Eq. 18 and consequently Eq. 19 become functions of the current density, thus allowing us to perform single variable optimization.

## V. RESULTS

In this section, the effect of current density upon the levelised cost of water, the efficiency and the membrane productivity of the hybrid system is presented. Table 3 provides the range of input values required for Eq. 19, allowing these values to be computed.

**Table 3: Cost Modelling Parameters**

Symbol	Value
$r$	10%
$T$	20 years
$CF$	0.9
$K_C$	\$1000/m <sup>2</sup> [5]
$K_E$	\$0.15/kWh
$S_c^A$	143 ppt
$S_d^A$	95 ppt
$S_c^B$	85 ppt
$S_d^B$	53 ppt

The return on capital should be selected in accordance with similar electro dialysis projects, of which there are few, if any, for high salinity hybrid ED-RO desalination. A moderate value of 10% is selected<sup>3</sup>. A moderate to high cost of electricity is selected to reflect poor grid connectivity if operated in remote locations. The capital cost per unit of cell pair area is approximated by quotations obtained by Oren et al. [5]. The mean concentrate and diluate salinities in ED systems A and B are computed via iteration over the current density between the hybrid system model and the cost model. Considering Eq. 19, increases in the return on capital or the capital cost per unit area would drive systems to higher optimal current densities, while increases in system lifetime, capacity factor and cost of energy would do the opposite.

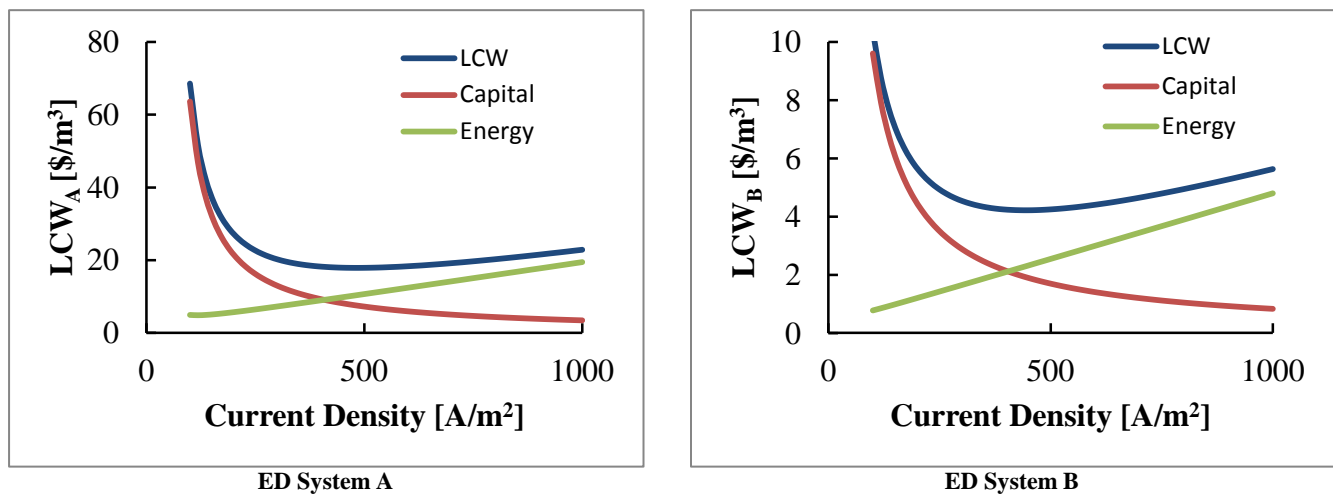


Figure 4. Impact of current density upon the levelised cost of water

Figs. 4A and 4B illustrate how the contribution of ED system A to the levelised cost of water (from the overall hybrid system) depends upon the current density. Of course, the total system cost should include the costs of systems A, B and the RO system. Figs. 5A and 5B illustrate the dependence of efficiency and membrane productivity upon current density. For both systems A and B, the LCW is minimised at a current density of approximately 500 A/m<sup>2</sup>. Capital costs are high at low current density due to low membrane productivity – little change in free energy of the streams is achieved per unit of membrane area. Conversely, at high current density the costs of energy dominate as efficiency decreases, due almost solely to the increased ohmic losses. The effects of efficiency and membrane productivity are easily visualised in Fig. 5.

<sup>3</sup> More rigorously, according to a capital asset pricing model, the rate of return should be consistent with the covariance of the project's cash flows with the returns of the overall financial markets. As a benchmark, as of 31<sup>st</sup> Jan 2013 3-year annualized returns on the S&P500 index were 14.14% [21]

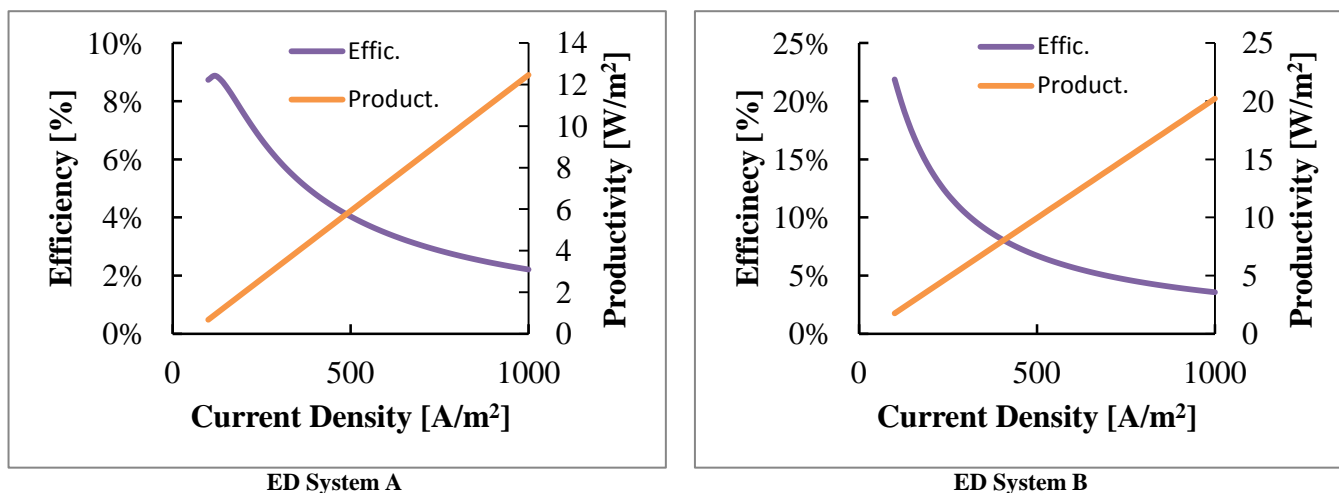


Figure 5. Impact of current density upon efficiency and membrane productivity

In Fig. 5A, it is seen that at low current there is a value of current density that maximises efficiency (though not the LCW). This optimum is explained by a balance of losses due to osmosis and ohmic resistance. At very low current density (below 100 A/m<sup>2</sup> in Fig. 5A), water transport via osmosis occurs rapidly relative to salt transport. By increasing the current density the relative effect of osmosis weakens. However, there is a competing trend whereby ohmic losses increase with current density – hence the presence of an optimum<sup>4</sup>.

Comparing Fig. 5A and Fig. 5B, it is noticeable that for the same current density the efficiency of system B is higher. This is explained by the lower average stream-to-stream concentration difference in unit B compared to unit A. In unit B, the effect of water transport via osmosis is less than in unit A. As a consequence, higher efficiencies are achievable in unit B and also the current density that maximises efficiency is smaller (and therefore not visible in Fig. 5B) than in unit A.

Of further interest is the fact that the current density maximising the LCW of units A and B is far above the current density maximising efficiency. Only with significant decreases in capital costs per unit membrane area, or significant increases in membrane properties such as conductivity (or decreases in water permeability) would the current density that maximises the LCW be driven towards the current density that maximises efficiency. This is in contrast to RO, which operates at a higher efficiency, indicating that the combination of capital costs per unit membrane area and membrane properties is superior to that in ED.

<sup>4</sup> Though efficiency exhibits an optimum, membrane productivity is monotonic in current density in this model as there is no competing factor reducing productivity at higher current density. Concentration polarization would constitute such a competing factor and its effect would be seen at high current densities, see Fig. 2.

**Table 4: Optimised system performance**

Symbol	Value
$\dot{V}_p$	100 m <sup>3</sup> /day
$RR_{RO}$	50%
$RR_{RO+EDB}$	29.5%
$RR_{hyb-sys}$	29%
$S_f$	120 ppt
$S_c$	167 ppt
$S_p$	0 ppt

**Table 5: Optimised system membrane areas and power consumption**

	ED A	ED B	RO
Membrane Area <sup>5</sup> [m <sup>2</sup> ]	240	100	90
Power Consumption [kWh/m <sup>3</sup> ]	43	21	6.1
LCW <sub>i</sub>	\$13/m <sup>3</sup>	\$4.3/m <sup>3</sup>	

In the optimized embodiment of the hybrid system, current densities are selected for systems A and B that minimize the contributions of those systems to the levelised cost of water. Tables 4 and 5 summarise key system characteristics. Of note is the finding that ED system A exhibits higher energy consumption and requires higher membrane area than ED system B. This is attributable to two factors. The reversible work done by system A is greater than that of B (on the basis of unit RO permeate production). This is due to the larger range of salinity covered by A compared with B. Secondly, the greater stream-to-stream concentration difference within A compared to B results in lower Second Law efficiency, due to a greater rate of water transport via osmosis.

The power consumption of the RO unit, though lower than the ED systems is high by SWRO standards, due to the absence of pressure recovery. Finally, the recovery ratio of the overall system is low, at 23%. It is possible to increase recoveries within system A by altering the relative mass flow rates of the unit. However, an increase in the stream-to-stream salinity difference would further decrease energy efficiency, membrane productivity and hence increase the LCW.

## VI. CONCLUSIONS

A hybrid arrangement of counterflow ED systems with reverse osmosis is presented. The premise of such an arrangement is to exploit ED for its ability to reach high osmotic pressures and exploit RO at low salinities where ohmic resistances are large in ED. The following specific conclusions are drawn:

- Contrary to brackish ED systems, membrane resistances dominate diluate and concentrate resistances in high salinity ED desalination.

<sup>5</sup> Total membrane area for RO, cell pair area for E<sup>-</sup>.

- The dominant factors influencing process efficiency and productivity are ohmic losses within membranes and losses of free energy due to water transport, each being relative to changes in free energy achieved in transporting salt from the diluate to the concentrated stream.
- At low current density capital costs dominate the LCW while energy costs dominate at high current density. The current density that minimises LCW is significantly greater than the current density that maximises efficiency, indicating the high current capital cost of ED per unit membrane area and poor membrane transport properties relative to RO.
- The efficiency of operation of an ED system depends significantly upon the stream-to-stream concentration with high values thereof increasing water transport via osmosis, decreasing efficiency and increasing the LCW. Consequently, the performance of ED systems achieving higher recoveries is significantly compromised.

In addition, the following areas meriting further analysis are exposed by the current work:

- The present analysis indicates that concentration polarization is not a significant factor given the low value of current densities minimising LCW. Consequently, larger membrane spacings appear achievable than in brackish water desalination, thus allowing significant reductions in the required pumping power. However, beyond the scope of the present contributions, an optimisation of ED pump systems is required to understand the trade-off between pumping power and concentration polarisation.
- There are few, if any, examples of counterflow ED systems for desalination at high salinity. Such a design allows the distinct advantage of maintaining a constant stream-to-stream concentration difference within stacks, thus maintaining a more constant current density and also rate of water transport. However, design issues such as the presence of trans-membrane pressures and leaking must be analysed carefully.

## VII. ACKNOWLEDGEMENTS

The first author would like to acknowledge support from the U.S. Department of State via the Fulbright Science and Technology Program, support from the MIT Martin Fellowship for Sustainability and support from IDA via the Channabasappa Memorial Scholarship. This research program is supported by King Fahd University of Petroleum and Minerals through the Center for Clean Water and Clean Energy at MIT and KFUPM.

## VIII. REFERENCES

1. Analysis, 2012. [desaldata.com](http://desaldata.com)
2. Water's growing role in oil and gas, 2011. Global Water Intelligence. URL: <http://www.globalwaterintel.com/archive/12/3/market-profile/waters-growing-role-oil-and-gas.html>
3. The desal revolution in a box, 2012. Global Water Intelligence. URL: <http://www.globalwaterintel.com/archive/13/3/market-profile/desal-revolution-box.html>
4. Korngold, E., L. Aronov, and N. Daltrophe. "Electrodialysis of brine solutions discharged from an RO plant." *Desalination* 242.1 (2009): 215-227.
5. Oren, Y., Korngold, E., Daltrophe, N., Messalem, R., Volkman, Y., Aronov, L., ... & Gilron, J. "Pilot studies on high recovery BWRO-EDR for near zero liquid discharge approach." *Desalination* 261.3 (2010): 321-330.

6. Thampy, S., Desale, G. R., Shahi, V. K., Makwana, B. S., & Ghosh, P. K. "Development of hybrid electro dialysis-reverse osmosis domestic desalination unit for high recovery of product water." *Desalination* 282 (2011): 104-108.
7. Casas, S., Bonet, N., Aladjem, C., Cortina, J. L., Larrotcha, E., & Cremades, L. V. "Modeling Sodium Chloride Concentration from Seawater Reverse Osmosis Brine by Electrodialysis: Preliminary Results." *Solvent Extraction and Ion Exchange* 29.3 (2011): 488-508.
8. Kwak, R.; Guan, G.; Peng, W. & Han, J. "Microscale electro dialysis: Concentration profiling and vortex visualization," *Desalination* 308 (2012): 138-146.
9. Bazant, M.; Kilic, M.; Storey, B. & Ajdari, A., "Towards an understanding of induced-charge electrokinetics at large applied voltages in concentrated solutions," *Advances in colloid and interface science*. 152.1 (2009): 48--88.
10. Nikonenko, V., Yaroslavtsev, A. B. and Pourcelly, P. "Structure, Properties and Theory". *Ion transfer in and through charged membranes* (2011).
11. Robinson, Robert Anthony, and Robert Harold Stokes. *Electrolyte solutions*. Dover Publications, 2002.
12. Kestin, J.; Khalifa, H. & Correia, R. *Tables of the dynamic and kinematic viscosity of aqueous NaCl solutions in the temperature range 20-150 °C and the pressure range 0.1-35 MPa*, (1981): American Chemical Society and the American Institute of Physics for the National Bureau of Standards.
13. Fidaleo, M. & Moresi, M., "Optimal strategy to model the electro dialytic recovery of a strong electrolyte", *Journal of membrane science* 260.1, (2005): 90--111.
14. Prentice, Geoffrey. *Electrochemical engineering principles*. Vol. 1. Englewood Cliffs, New Jersey: Prentice Hall, 1991.
15. Berezina, N.; Gnusin, N.; Dyomina, O. & Timofeyev, S., "Water electrotransport in membrane systems. Experiment and model description," *Journal of membrane science* 86.3, (1994): 207--229.
16. Helfferich, Friedrich. *Ion exchange*. Dover Publications, 1995.
17. Neosepta. ASTOM Corporation. URL: <http://www.astom-corp.jp/en/en-main2-neosepta.html>, [accessed 2013.15.02].
18. Fidaleo, Marcello, and Mauro Moresi. "Electro dialytic desalting of model concentrated NaCl brines as such or enriched with a non-electrolyte osmotic component." *Journal of Membrane Science* 367.1 (2011): 220-232.
19. Wilf, Mark, and Leon Awerbuch. *The guidebook to membrane desalination technology*. L'Aquila, Italy: Balaban Desalination Publications, (2007).
20. Busey, R. H. "Thermodynamic Properties of Aqueous-Sodium Chloride Solutions." *J. Phys. Chem. Ref. Data* 13.1 (1984).
21. Standard and Poor. S&P 500 Performance Data. URL: <http://www.standardandpoors.com/indices/sp-500/en/us/?indexId=spusa-500-usdof--p-us-l--> [accessed 2013.02.19]